Effect of correlations and doping on the spin susceptibility of iron pnictides: the case of KFe_2As_2

S. L. Skornyakov[+,*], *V. I. Anisimov*[+,*], *and D. Vollhardt*[×]

[+] *Institute of Metal Physics, Russian Academy of Sciences, S. Kovalevskaya Str. 18, 620990 Yekaterinburg, Russia*
[*] *Ural Federal University, 620002 Yekaterinburg, Russia*
[×] *Theoretical Physics III, Center for Electronic Correlations and Magnetism, Institute of Physics, University of Augsburg, D-86135 Augsburg, Germany*

July 28, 2014

arXiv:1401.6291v3 [cond-mat.str-el] 25 Jul 2014

The temperature dependence of the paramagnetic susceptibility of the iron pnictide superconductor KFe_2As_2 and its connection with the spectral properties of that material is investigated by a combination of density functional theory (DFT) in the local density approximation and dynamical mean-field theory (DMFT). Unlike other iron pnictide parent compounds where the typical oxidation state of iron is 2, the formal valence of Fe in KFe_2As_2 is 2.5, corresponding to an effective doping with 0.5 hole per iron atom compared to, for example, $BaFe_2As_2$. This shifts the chemical potential and thereby reduces the distance between the peaks in the spectral functions of KFe_2As_2 and the Fermi energy as compared to $BaFe_2As_2$. The shift, which is clearly seen on the level of DFT as well as in DMFT, is further enhanced by the strong electronic correlations in KFe_2As_2. In $BaFe_2As_2$ the presence of these peaks results [Phys. Rev. B **86**, 125124 (2012)] in a temperature increase of the susceptibility up to a maximum at ~ 1000 K. While the temperature increase was observed experimentally the decrease at even higher temperatures is outside the range of experimental observability. We show that in KFe_2As_2 the situation is different. Namely, the reduction of the distance between the peaks and the Fermi level due to doping shifts the maximum in the susceptibility to much lower temperatures, such that the decrease of the susceptibility becomes visible in experiment.

Introduction. The discovery of high-temperature superconductivity in fluorine-doped LaFeAsO in 2008 by Kamihara et al. [1] has placed the iron-arsenic systems into the center of activity of solid state physics. To date a variety of Fe-based superconductors have been found. The so-called '122' family (compounds with the common formula $AEFe_2As_2$, where AE=alkaline earth element) is the most studied one. Unlike other iron-arsenic systems, undoped compounds of the '122' family superconduct under pressure, with T_c up to 29 K [2, 3]. The highest critical temperature, T_c = 38 K, in this family is detected in the potassium doped compound $Ba_{1-x}K_xFe_2As_2$ with $x = 0.4$ [4, 5, 6]. Therefore KFe_2As_2 is the end member of the family and can be considered a parent compound in which superconductivity emerges under chemical doping. Although the critical temperature is rather low in KFe_2As_2 (T_c=3.8 K [7]) this material is a rare example of a stoichiometric pnictide superconductor.

It is widely accepted that Coulomb correlations are crucial for the understanding of many aspects of the physics of pnictides [9, 10, 11, 8]. Correlation effects in KFe_2As_2 were intensively studied: Terashima et al. [12] performed de Haas-van Alphen measurements of the Fermi surface in KFe_2As_2. They detected unusually large effective mass renormalizations and big differences in the masses of different bands, which is not found in other pnictides. The enhancement of the band mass was also measured by Yoshida et al. [13] in angular-resolved photoemission spectroscopy (ARPES) experiments. Hardy et al. [14] employed the Gutzwiller slave-boson mean-field method to study the strength of Coulomb correlations in KFe_2As_2. They confirmed the experimental conclusions of Terashima et al. [12] and Yoshida et al. [13], and proposed an orbital-selective scenario for its spectral properties.

A characteristic feature of the magnetic properties observed in the '1111' (compounds like LaFeAsO) and '122' pnictide classes is the unusual linear-temperature increase of the paramagnetic susceptibility [15, 16]. There are two explanations of this phenomenon based either on the assumption of strong antiferromagnetic fluctuations in a two-dimensional Fermi liquid [17], or of peculiarities of the single-particle spectra [10, 11]. The temperature increase of the susceptibility was considered a universal property [18] of the pnictide superconductors and parent systems. By contrast, Cheng et al. [19] reported that in KFe_2As_2 the magnetic susceptibility increases only at quite low temperatures, i.e., below 100 K, and then decreases slowly at least up to 300 K. The origin of that temperature dependence of the magnetic susceptibility of KFe_2As_2 and its connection with the magnetic properties of the other end member of the '122' family, $BaFe_2As_2$, had not been

explained yet. In particular, it was not studied by first-principle methods.

Today the most powerful technique that can account for correlation effects in real compounds and can describe the physics of the correlated paramagnetic phase, is the LDA+DMFT approach [20]. This method combines the advantage of density-functional theory (typically in the local density approximation (LDA)) to describe the material-specific electronic structure of a weakly correlated system, with the ability of the dynamical mean-field theory [21] to treat the complete range of Coulomb correlations between the electrons in partially filled shells.

In this work, we investigate the temperature evolution of the paramagnetic susceptibility in KFe_2As_2 in the framework of LDA+DMFT. We compare our results with experiments and our previously published LDA+DMFT data [11] obtained for the isostructural compound $BaFe_2As_2$. Thereby we demonstrate that the mechanism explaining the anomalous temperature behavior of the magnetic susceptibility in iron pnictides proposed in our previous investigations [10, 11] also allows one to understand the difference between the magnetic properties of these compounds and those of KFe_2As_2.

Technical details. In the LDA+DMFT formalism employed here the material-specific band dispersion obtained within LDA is used as a starting point. Then matrix elements of the effective Hamiltonian $H^{\mathrm{LDA}}(\mathbf{k})$ are computed in the subspace of Wannier functions with the symmetry of p and d states using the projection procedure [22]. In the second step, the Coulomb interaction matrix $U^{\sigma\sigma'}_{mm'}$, parametrized by Slater integrals F_0, F_2 and F_4, is calculated for each atom with partially filled shells. The values of F_0, F_2, F_4 are computed using the on-site effective Coulomb parameter U and intraatomic exchange parameter J. Finally, the following many-electron Hamiltonian is iteratively solved by DMFT on the Matsubara contour:

$$\hat{H}(\mathbf{k}) = \sum_{\mathbf{k},im,jm',\sigma} (H^{\mathrm{LDA}}_{im,jm'}(\mathbf{k}) - H^{\mathrm{DC}}_{im,jm'})\hat{a}^{\dagger}_{\mathbf{k},im\sigma}\hat{a}_{\mathbf{k},jm'\sigma} + \frac{1}{2}\sum_{i,(m\sigma)\neq(m'\sigma')} U^{\sigma\sigma'}_{mm'}\hat{n}^{d}_{im\sigma}\hat{n}^{d}_{im'\sigma'}. \quad (1)$$

Here $\hat{a}^{\dagger}_{\mathbf{k},im\sigma}$ is the Fourier transform of $\hat{a}^{\dagger}_{im\sigma}$ which creates an electron on the atom i in the state $|m\sigma\rangle$, where m labels the orbitals and $\sigma =\uparrow,\downarrow$ corresponds to the spin projection. The particle number operator $\hat{n}^{d}_{im\sigma}$ acts on the states localized at the atoms with partially filled shells (Fe-d states in the present study). The term H^{DC} stands for a double-counting correction which corresponds to the Coulomb interaction energy already accounted for by LDA (see below).

In the present work the LDA band structure is calculated with the ELK full-potential code [23] with default parameters of the LAPW basis. By employing the constrained LDA method [24] we obtained the interaction parameters $U = 3.5$ eV and $J = 0.85$ eV. These values are typical for the pnictides and are in good agreement with previous estimations [9, 25]. The DMFT auxiliary impurity problem was solved by the hybridization function expansion quantum Monte-Carlo method [26]. The double-counting term is a diagonal matrix with only nonzero elements in the $d-d$ block expressed in the form $E^{\mathrm{DC}} = \bar{U}(n_d - 0.5)$, where n_d is the number of Fe-d electrons calculated within LDA+DMFT and $\bar{U}$ is the average Coulomb parameter for the d states. This form of H^{DC} yields reliable results for magnetic and spectral properties of iron pnictides [10, 11, 8, 9].

The orbitally-resolved spectral functions $A_i(\omega)$ were computed as the diagonal elements of the real-energy Green function

$$A_i(\omega) = \sum_{\mathbf{k}}[I(\omega+\mu) - (H^{\mathrm{LDA}}(\mathbf{k}) - H^{\mathrm{DC}}) - \Sigma(\omega)]^{-1}_{ii}, \quad (2)$$

where μ is the chemical potential calculated within DMFT, $\Sigma(\omega)$ is the self-energy obtained with the use of Padé approximants [27], and I is the identity matrix.

The uniform magnetic susceptibility $\chi(T)$ was calculated as the response to a small external magnetic field,

$$\chi(T) = \frac{\Delta M(T)}{\Delta E}, \quad (3)$$

where ΔE is the energy correction corresponding to the field and $\Delta M = |N_{\uparrow}(T) - N_{\downarrow}(T)|$ is the occupation difference between the spin projections.

Temperature dependence of the uniform magnetic susceptibility. In the upper panel of Fig.1 the temperature behavior of the static magnetic susceptibility of KFe_2As_2 as computed within LDA+DMFT is shown in comparison with the experimental result of Cheng et al. [19]. Both experimental and theoretical curves show a monotonic decrease in the temperature interval from 125 to 300 K. The slope of the calculated curve is in good agreement with experiment, while its absolute value is by about 20% smaller. The maximum in the experimental susceptibility observed at 100 K is not reproduced in the calculation. Temperatures lower than 77 K are not accessible in the present study. The temperature dependence of the LDA+DMFT calculated paramagnetic susceptibility in the other

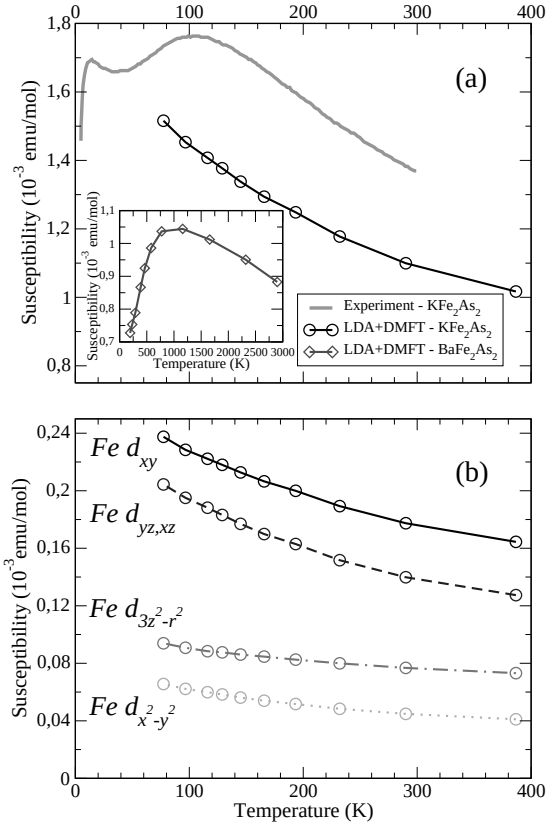

Fig.1. Temperature dependence of the uniform susceptibility of KFe_2As_2. (a) The static susceptibility as a function of temperature computed within LDA+DMFT (circles) is shown in comparison with experimental data of Cheng et al. [19] (solid curve). The inset shows the LDA+DMFT result for the susceptibility of $BaFe_2As_2$ from Ref. [11]. (b) Temperature behavior of the orbitally-resolved contributions to the total susceptibility calculated by LDA+DMFT

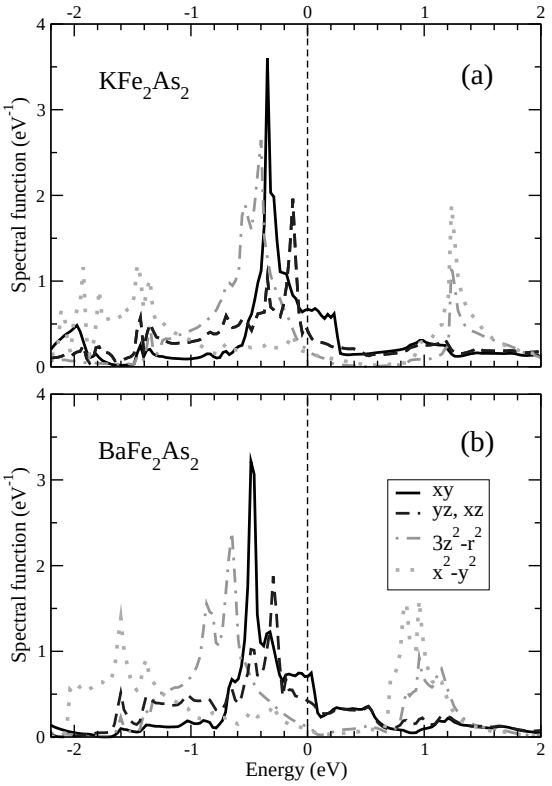

Fig.2. Fe-d orbitally-resolved densities of states of KFe_2As_2 (a) and $BaFe_2As_2$ (b) obtained within LDA (0 eV corresponds to the Fermi energy)

end member of the '122' family is shown in the inset of Fig.1. The similarities and differences of the curves are discussed in the Discussion section. The orbitally resolved Fe-d contributions to the total susceptibility are presented in the lower panel of Fig.1. The susceptibilities corresponding to the Fe-d orbitals all show a decreasing behavior with temperature. The largest contributions come from the xy and $yz(xz)$ orbitals.

Spectral properties. The orbitally resolved densities of states of KFe_2As_2 obtained within LDA are shown in the upper panel of Fig.2 in comparison with the result obtained for $BaFe_2As_2$. In each case the Fe-d states form a band with total width of $W \approx 4$ eV located in the approximate interval $(-2, +2)$ eV. Therefore the on-site Coulomb parameter U is comparable with the band width ($W/U \sim 1$), implying that correlation effects are important. Both compounds have similar shape and relative positions of the spectral functions on the energy axis. However, in the case of KFe_2As_2 the Fermi level is located approximately 150 meV lower than in $BaFe_2As_2$ due to hole doping.

The Fe-d spectral functions of KFe_2As_2 computed within LDA+DMFT for the temperature window from 77 to 580 K are presented in Fig.3 along with the result for $BaFe_2As_2$ [11]. As in other pnictide superconductors the dynamical Coulomb correlations renormalize the spectrum in the vicinity of the Fermi energy and smear some fine details observed within the LDA, but the overall shape of the curves remains unchanged. This renormalization reduces the distance between the peaks in the Fe-d spectral functions and the Fermi energy. In particular, the peak in the $yz(xz)$ spectral function is now significantly closer to the Fermi level compared to that in $BaFe_2As_2$.

Quantitatively, the strength of the electronic correlations can be estimated by the increase of the effective masses in comparison with the LDA results. In the case of a single orbital the mass renormalization is expressed by the derivative of the self-energy $\Sigma(\omega)$

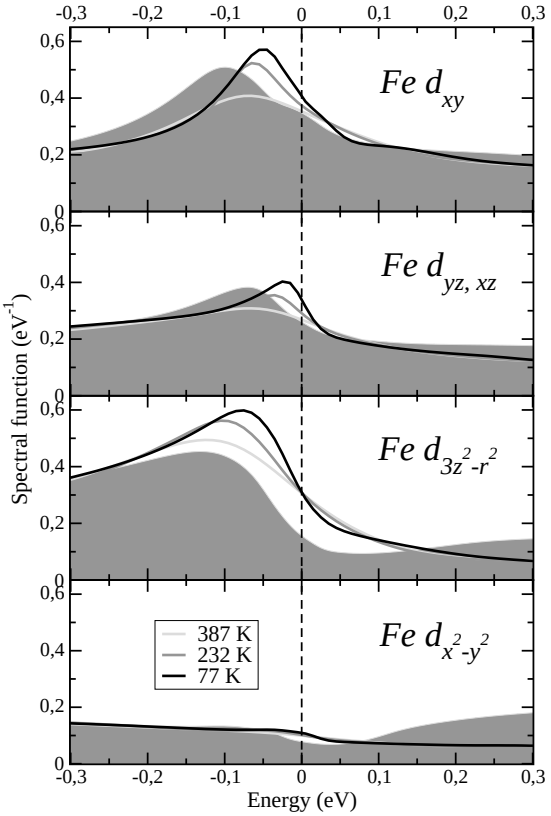

Fig.3. Temperature evolution of Fe-d spectral functions of KFe_2As_2 computed by LDA+DMFT. The spectral functions of $BaFe_2As_2$ corresponding to the temperature T=232 K taken from Ref. [11] are shown for comparison as shaded areas. The Fermi energy is set to 0 eV

as $m^*/m_b = (1 - \partial \mathrm{Re}\Sigma(\omega)/\partial\omega)$, where m^* denotes the effective mass in LDA+DMFT and m_b is the band mass obtained in LDA. In our calculation the self-energy is a diagonal matrix which leads to an orbital dependence of the masses. The calculated values of m^*/m_b for every Fe-d orbital are shown in Table.2. The largest mass renormalization, 4.47, corresponds to the xy orbital. Electronic correlations in the other d-orbitals are weaker with m^*/m_b ranging from 2.22 to 4.02. The computed values of m^*/m_b are in good agreement with previous theoretical estimations [14] as well as with the ARPES data of Yoshida et al. [13]. The result that the electrons in the $|xy\rangle$-derived bands are the most correlated ones followed by the $|yz\rangle$, $\left|3z^2 - r^2\right\rangle$, and $\left|x^2 - y^2\right\rangle$ states, is in qualitative agreement with the conclusion on the proximity of KFe_2As_2 to an orbital-selective Mott transition reported by Hardy et al. [14]. It should also be noted that the response of the electrons occupying states with larger m^*/m_b is more Curie-Weiss-like, while the temperature dependence of the susceptibilities corresponding to the other orbitals is less prononunced. A similar result was obtained in Ref. [28] for the local susceptibility of LaFeAsO.

Table I. The effective mass enhancement m^*/m_b for different orbitals of the d shell

	d_{xy}	d_{yz}	$d_{3z^2-r^2}$	$d_{x^2-y^2}$
m^*/m	4.74	4.02	2.96	2.22

Discussion. To explain why the magnetic susceptibility of KFe_2As_2 behaves qualitatively different from that of the other iron pnictides it is instructive to compare the spectral properties of KFe_2As_2 and the other end member of the '122' family, $BaFe_2As_2$. As noted above, in KFe_2As_2 the Fermi energy is lower than in $BaFe_2As_2$ due to hole doping. Already on the level of LDA this results in a smaller distance between the peaks of the Fe-d spectral functions and the Fermi energy. Since correlation effects in KFe_2As_2 are stronger than in $BaFe_2As_2$ the peaks obtained within LDA+DMFT come to lie even closer to the Fermi energy. This is clearly seen in Fig.3 where the orbitally resolved Fe-d spectral functions of $BaFe_2As_2$ are shown for comparison.

In our previous study [11] we investigated the temperature behavior of the magnetic susceptibility in a model where the spectral function has a sharp peak below the Fermi energy. It was shown that the behavior of the magnetic susceptibility is determined by the thermal excitations corresponding to the states forming the peak, and that the distance between the peak and the Fermi energy can be regarded as a parameter controlling the magnetic response of the system. According to the present LDA+DMFT study, in KFe_2As_2 the peaks of the Fe-d spectral functions are significantly closer to the Fermi energy than in $BaFe_2As_2$. Physically this means that the excitation of the states forming the peaks in KFe_2As_2 requires less energy than in $BaFe_2As_2$. An analysis of the model shows that the doping of 0.5 holes per iron atom is not sufficient to switch the system to the regime where the linear in T behavior of the susceptibility no longer exists. Therefore we expect the linear increase of $\chi(T)$ of KFe_2As_2 to start at a lower temperature than in $BaFe_2As_2$, while the overall shape of the susceptibility curves is similar. Indeed, the decreasing part of the experimentally measured susceptibility of KFe_2As_2 is well described by our result.

We were not able to perform the susceptibility calculations for temperatures lower than 77 K because Monte-Carlo simulations become extremely time

consuming. As a consequence the maximum of the susceptibility in KFe_2As_2 is not captured by our calculations. In our previous investigation we showed that the increasing part of the curve below that maximum can be interpreted as a quasilinear region in the vicinity of a turning point. In KFe_2As_2 a similar region is experimentally observed in the temperature window from 30 to 80 K. It remains to be seen whether this low-temperature behavior can be explicitly reproduced in future LDA+DMFT studies.

In conclusion, the temperature dependence of the uniform magnetic susceptibility of KFe_2As_2 was investigated within the LDA+DMFT method. The temperature decrease of the computed susceptibility between 125 K to 300 K agrees well with experiment. We found that, similar to other pnictides including the isostructural parent compound $BaFe_2As_2$, the Fe-d spectral functions of KFe_2As_2 show sharp peaks below the Fermi energy. However, these peaks lie significantly closer to the Fermi level than in $BaFe_2As_2$. Making use of the scenario developed in our previous study of the magnetic properties of iron pnictides, we conclude that the qualitative difference between the magnetic susceptibilities of the two isostrucural end members of the '122' family is due to the smaller separation between the Fe-d spectral functions and the Fermi energy in KFe_2As_2, which itself is a consequence of the effective hole doping and the stronger correlations in that compound.

This work was supported by the Russian Foundation for Basic Research (Projects No. 13-02-00050-a, No. 13-03-00641-a) and the Ural Division of the Russian Academy of Science Presidium (Project No. 14-2-NP-164, No. 12-P2-1017). S.L.S. is grateful to the Dynasty Foundation for support. S.L.S and V.I.A. are grateful to the Center for Electronic Correlations and Magnetism, University of Augsburg for hospitality. This work was supported in part by the Deutsche Forschungsgemeinschaft through Transregio TRR 80. All results reported here were obtained using "Uran" supercomputer of IMM UB RAS.

1. Y. Kamihara et al., J. Am. Chem. Soc. **128**, 10012 (2006).
2. A. Kreyssig et al., Phys. Rev. B **78**, 184517 (2008).
3. Patricia L. Alireza et al., J. Phys. Condens. Matter **21**, 012208 (2009).
4. M. Rotter et al., Phys. Rev. Lett. **101**, 107006 (2008).
5. H. Chen et al., Europhys. Lett. **85**, 17006 (2009).
6. K. Sasmal et al., Phys. Rev. Lett. **101**, 107007 (2008).
7. K. Kihou et al., J. Phys. Soc. Jpn. **79**, 124713 (2010).
8. S. L. Skornyakov et al., Phys. Rev. B **81**, 174522 (2010).
9. M. Aichhorn et al., Phys. Rev. B **80**, 085101 (2009).
10. S. L. Skornyakov et al., Phys. Rev. Lett. **106**, 047007 (2011).
11. S. L. Skornyakov et al., Phys. Rev. B **86**, 125124 (2012).
12. T. Terashima et al., Journal of the Physical Society of Japan **79**, 053702 (2010).
13. T. Yoshida et al., J. Phys. Chem. Solids **72**, 465 (2011).
14. F. Hardy et al., Phys. Rev. Lett **111**, 027002 (2013).
15. X. F. Wang et al., Phys. Rev. Lett. **102**, 117005 (2009).
16. R. Klingeler et al., Phys. Rev. B **81**, 024506 (2010).
17. M. M. Korshunov et al., Phys. Rev. Lett. **102**, 236403 (2009).
18. G. M. Zhang et al., Europhys. Lett. **86**, 37006 (2009).
19. B. Cheng et al., Phys. Rev. B **86**, 134503 (2012).
20. V. I. Anisimov et al., J. Phys.: Condens. Matter **9**, 7359 (1997); A. I. Lichtenstein et al., Phys. Rev. B **57**, 6884 (1998); K. Held et al., Phys. Status Solidi B **243**, 2599 (2006); G. Kotliar et al., Rev. Mod. Phys. **78**, 865 (2006); K. Held, Adv. Phys. **56**, 829 (2007).
21. W. Metzner et al., Phys. Rev. Lett. **62**, 324 (1989); A. Georges et al., Rev. Mod. Phys. **68**, 13 (1996).
22. V. I. Anisimov et al., Phys. Rev. B **71**, 125119 (2005).
23. http://elk.sourceforge.net/.
24. A. I. Liechtenstein et al., Phys. Rev. B **52**, 5467R (1995).
25. V. I. Anisimov et al., J. Phys.: Condens. Matter **21** 075602 (2009).
26. P. Werner et al., Phys. Rev. Lett. **97**, 076405 (2006).
27. H. J. Vidberg et al., J. Low Temp. Phys. **29**, 179 (1977).
28. K. Haule et al., New Journal of Physics **11**, 025021 (2009).